Supporting Information

Significantly Reduced Thermal-Activation Energy for Hole Transport via Simple Donor Engineering: Understanding the Role of Molecular Parameters for Thermoelectric Behaviors

Fei Zhong,[†,#] Xiaojun Yin,[†,#] Zhanxiang Cheng,[‡] Chunmei Gao[§] and Lei Wang[†,]*

[†]Shenzhen Key Laboratory of Polymer Science and Technology, College of Materials Science and Engineering, Shenzhen University, Shenzhen 518060, China. E-mail: wl@szu.edu.cn

[‡]Hubei Key Lab on Organic and Polymeric Optoelectronic Materials, Department of Chemistry, Wuhan University, Wuhan, 430072, P. R. China.

[§]College of Chemistry and Chemical Engineering, Shenzhen University, Shenzhen 518060, PR China.

[#]These authors contribute equally to this work.

Table of contents

General Information for Characterization and Measurements

^{1}H NMR spectra of the polymers in $CDCl_3$ were recorded on a Bruker ADVANCE Ⅲ nuclear magnetic resonance spectrometer (600 MHz) with tetramethylsilane as the internal standard. The number-average molecular weights (M_n) and polydispersity indexes (PDI) of samples distribution of the polymer were determined by gel permeation chromatography (GPC) system (Waters e2695 Separations Module, Waters, Singapore). Thermogravimetric measurements (TGA) was carried out by using a TGA-Q50 under a nitrogen atmosphere with a heating rate of 10 °C/min. Differential Scanning Calorimetry (DSC) was measured under a nitrogen atmosphere using a DSC 7020 (Hitachi) apparatus equiped with a liquid nitrogen cooling system. UV-vis-NIR absorption spectra of polymer films and solutions were measured on a PerkinElmer Lambda 950 spectrophotometer. Cyclic voltammetry (CV) experiments were taken on a CHI 660 workstation. The polymer film was measured in acetonitrile solution with tetrabutylammonium hexafluorophosphate (0.1 M) as the electrolyte. The platinum disk electrode was used as the working electrode and the platinum wire was used as the counter electrode, and the Ag / AgCl electrode was used as the reference electrode with ferrocenium-ferrocene (Fc^+/Fc) as the internal standard. The scanning rate was 50 mV s^{-1} under the nitrogen atmosphere. Grazing Incidence X-ray Diffraction (GIXRD) were collected on an X-ray diffractometer (SmartLab, Japan) with a Cu target (λ = 1.54 Å). Diffraction patterns were obtained at a scan rate of 5° min^{-1}. The surface morphologies of polymer films were observed by scanning electron microscopy (SEM, S-4700, Hitachi). The elemental analysis for these polymer films were obtained by the area scanning of energy dispersive spectroscopy (EDS, Oxford X-Max^N). The electron binding energy was measured on an X-ray photoelectron spectrometer （XPS, K-Alpha$^+$, Thermo Fisher Scientific). Ultraviolet photoemission spectroscopy (UPS） data was collected using an ESCALAB

250Xi X-ray photoelectron spectrometer with a He I (21.22 eV) gas discharge lamp source and a monochromatic Al Kα source as the excitation source.

Materials and Syntheses

Materials

All commercially available reagents were used directly unless otherwise noted. $Pd(pph_3)_4$, $Pd_2(dba)_3$, $P(o\text{-}tol)_3$, and anhydrous $FeCl_3$ were obtained from Sun Chemical Technology Co. Ltd (Shanghai, China). 9-octyl-2,7-bis(4,4,5,5-tetramethyl-1,3,2-dioxaborolan-2-yl)-9*H*-carbazole and 4-octyl-2,6-bis(trimethylstannyl)-4*H*-dithieno[3,2-b:2',3'-d] pyrrole was purchased from Sun Tech Inc. (Suzhou, China). 3,6-bis(5-bromothiophen-2-yl)-2,5-bis(2-octyldodecyl)-2,5-dihydropyrrolo[3,4-*c*] pyrrole-1,4-dione was purchased from Derthon Optoelectronic Materials Science Technology Co. Ltd. (Shenzhen, China).

Synthesis of PCZ-DPP

9-octyl-2,7-bis(4,4,5,5-tetramethyl-1,3,2-dioxaborolan-2-yl)-9*H*-carbazole (150.0 mg, 0.28 mmol), 3,6-bis(5-bromothiophen-2-yl)-2,5-bis(2-octyldodecyl)-2,5-dihydropyrrolo[3,4-*c*] pyrrole-1,4-dione (287.7 mg, 0.28 mmol) and $Pd(PPh_3)_4$ (3% , 9.8 mg) were added to a Schlenk flask. Subsequently, a mixed solution of THF (8 ml) and 2 mol/L aqueous solution of K_2CO_3 (4 ml) were added. The Schlenk flask was continuously purged with nitrogen for 30 minutes to achieve an oxygen-free atmosphere, and then mixture solution was stirred and heated to 85 ℃ for 72 h. After the mixture was cooled to room temperature, the mixture was slowly poured into methanol to precipitated the polymer. The precipitate was collected and washed further with methanol, acetone and hexane to remove oligomers and other impurities. The solid was dissolved in $CHCl_3$ (100 mL) and dried over $MgSO_4$. The concentrated solution was reduced to 20-30 ml under reduced pressure and precipitated in methanol. The resulting polymer was finally dried under vacuum overnight. The purified polymer was obtained as

dark brown solid (229 mg, yield 72%). ^{1}H NMR (600 MHz, $CDCl_3$) [ppm]: 9.02 (br, 2H), 7.97 (br, 2H), 7.72-6.80 (m, 6H), 2.14 -1.03 (m, 78H), 0.78-0.96 (m, 15H).

Synthesis of PDTP-DPP

4-octyl-2,6-bis(trimethylstannyl)-4*H*-dithieno[3,2-b:2',3'-d]pyrrole(162.4 mg, 0.26 mmol), 3,6-bis(5-bromothiophen-2-yl)-2,5-bis(2-octyldodecyl)-2,5-dihydropyrrolo[3,4-c]pyrrole-1,4-dione(268.2 mg, 0.26 mmol), $Pd_2(dba)_3$ (5%, 12.1 mg) and $P(o\text{-}tol)_3$ (25%, 20 mg) were added to a Schlenk flask. Subsequently, anhydrous chlorobenzene (8 ml) was injected into the Schlenk flask with a syringe. The Schlenk flask was continuously purged with nitrogen for 30 minutes to achieve an oxygen-free atmosphere, and then mixture solution was stirred and heated to 110 ℃ for 72 h. After the mixture was cooled to room temperature, the mixture was slowly poured into methanol to precipitated the polymer. The precipitate was collected and washed further with methanol, acetone and hexane to remove oligomers and other impurities. The resulting polymer was finally dried under vacuum overnight. The purified polymer was obtained as deep purple solid (224 mg, yield 75%). ^{1}H NMR (600 MHz, $CDCl_3$) [ppm]: 8.98 (br, 2H), 7.5-6.7 (m, 4H), 4.06 (br, 6H), 2.05-1.02 (m, 78H), 0.96-0.68 (m, 15H).

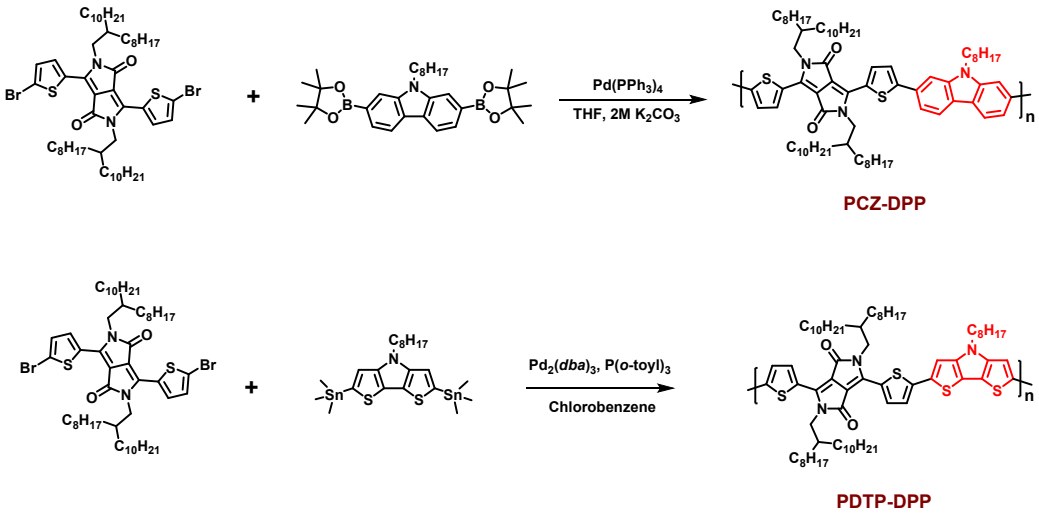

Scheme S1. Synthetic route of PCZ-DPP and PDTP-DPP.

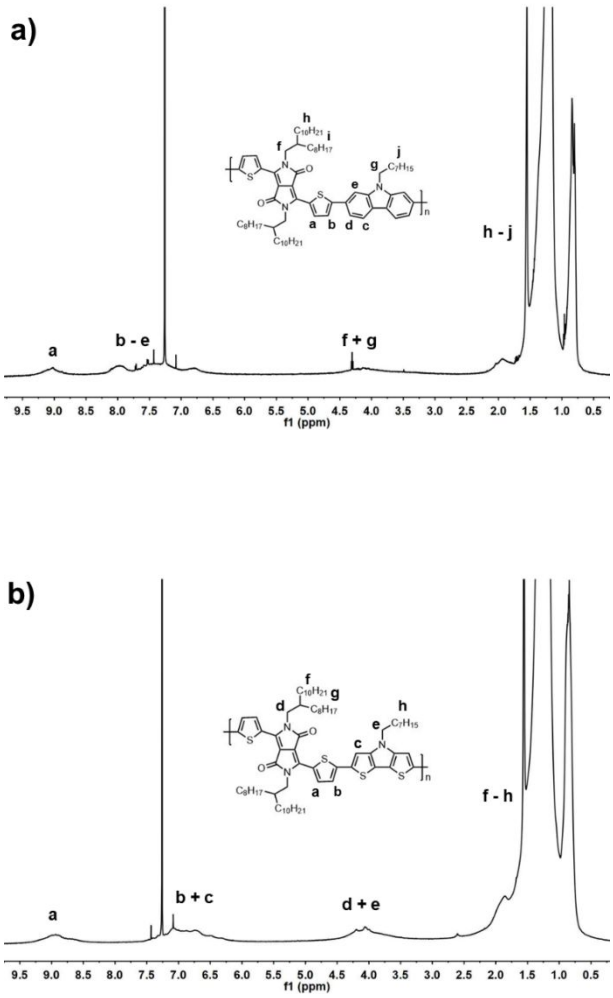

Figure S1. ^{1}H NMR spectra of a) the PCZ-DPP and b) the PDTP-DPP.

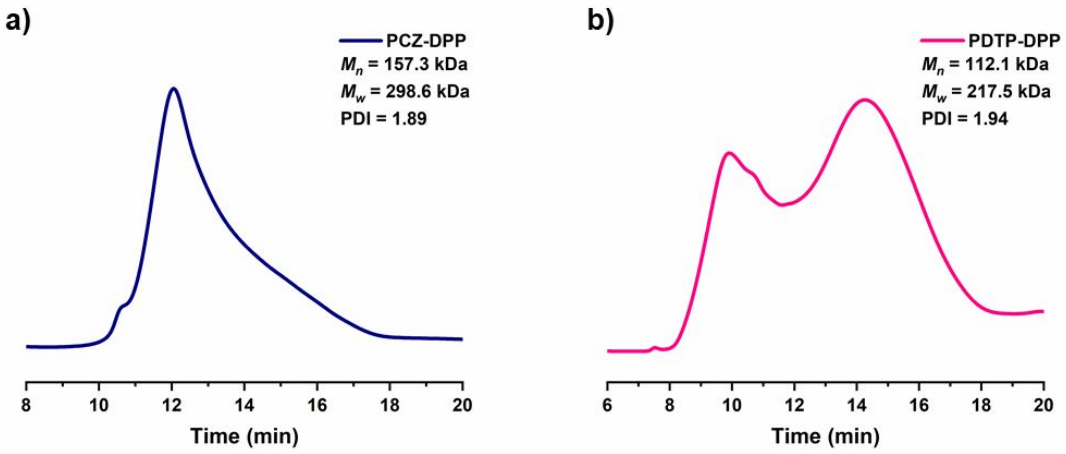

Figure S2. Molecular weights and polymer dispersity index measured from gel permeation chromatography, a) for PCZ-DPP and b) for PDTP-DPP.

Thermal, photophysical, and electrochemical properties of the polymers

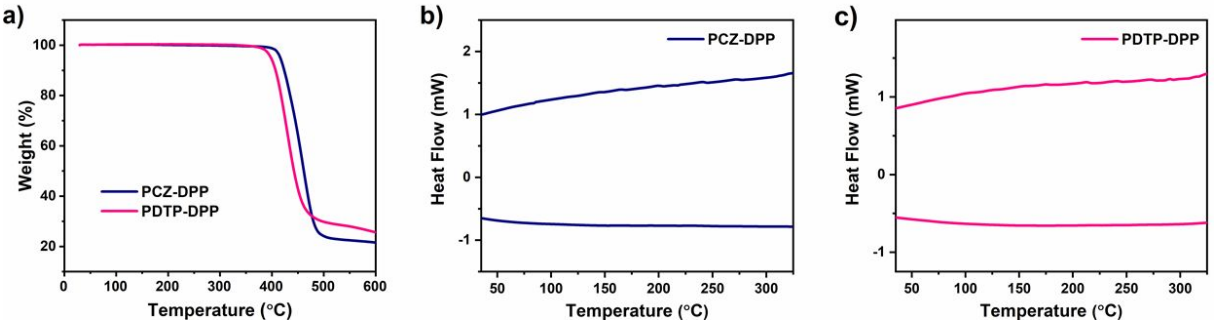

Figure S3. a) Thermal gravity analysis, and differential scanning calorimeter traces of b) the PCZ-DPP and c) the PDTP-DPP.

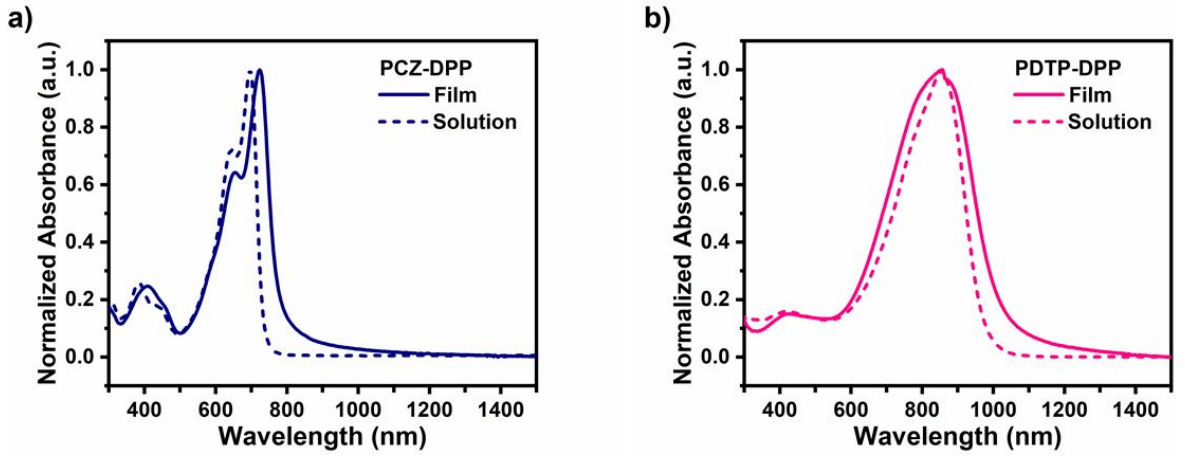

Figure S4. Normalized UV-vis-NIR absorption spectra of a) PCZ-DPP and b) PDTP-DPP both in solution and thin-film states.

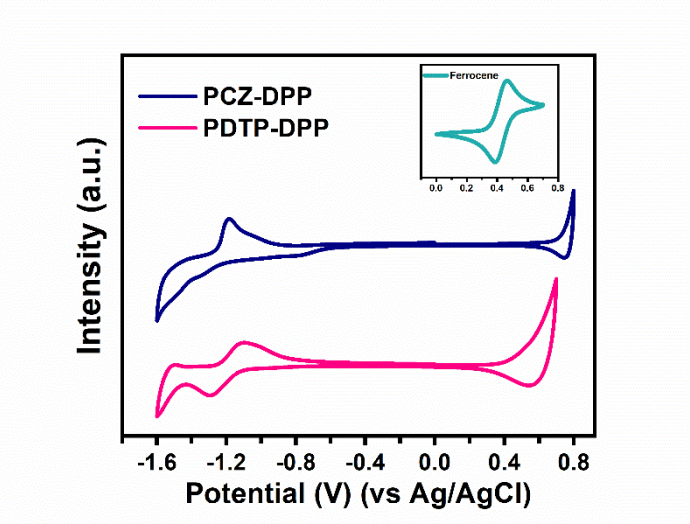

Figure S5. Cyclic voltammograms curves of the PCZ-DPP and PDTP-DPP.

Density functional theory calculations

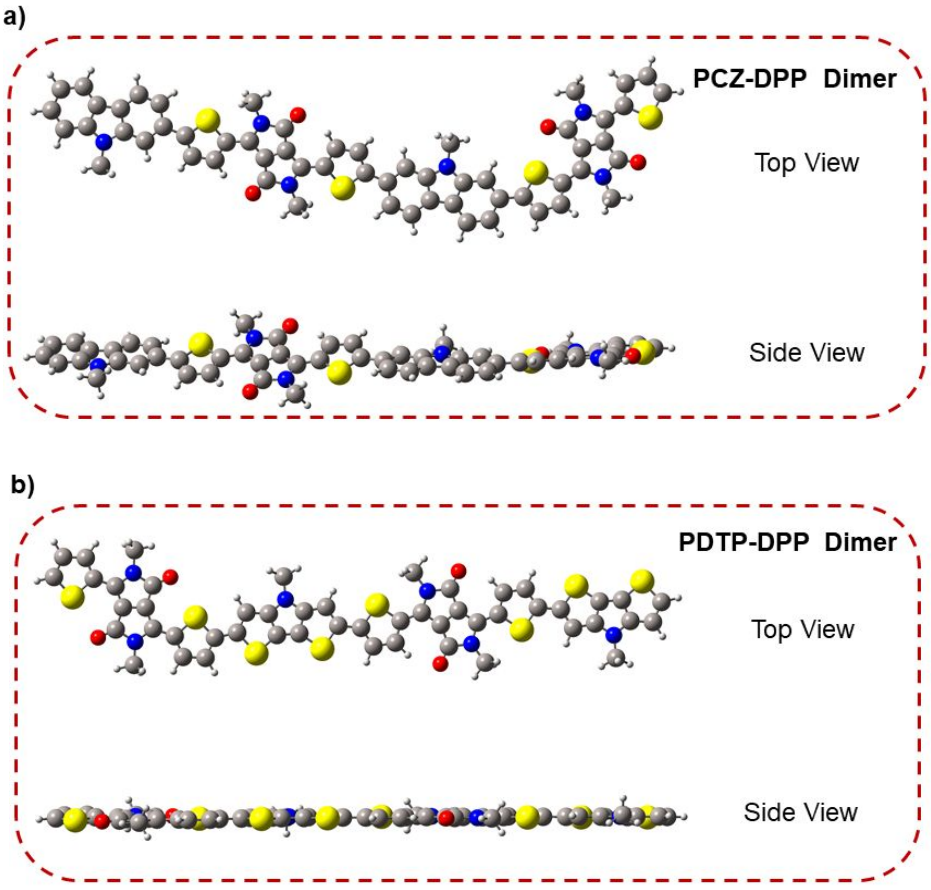

Figure S6. Optimized geometries of the dimers for a) the PCZ-DPP and b) the PDTP-DPP, and the long alkyl chains were replaced with methyl groups to simplify calculation.

Thermoelectric properties

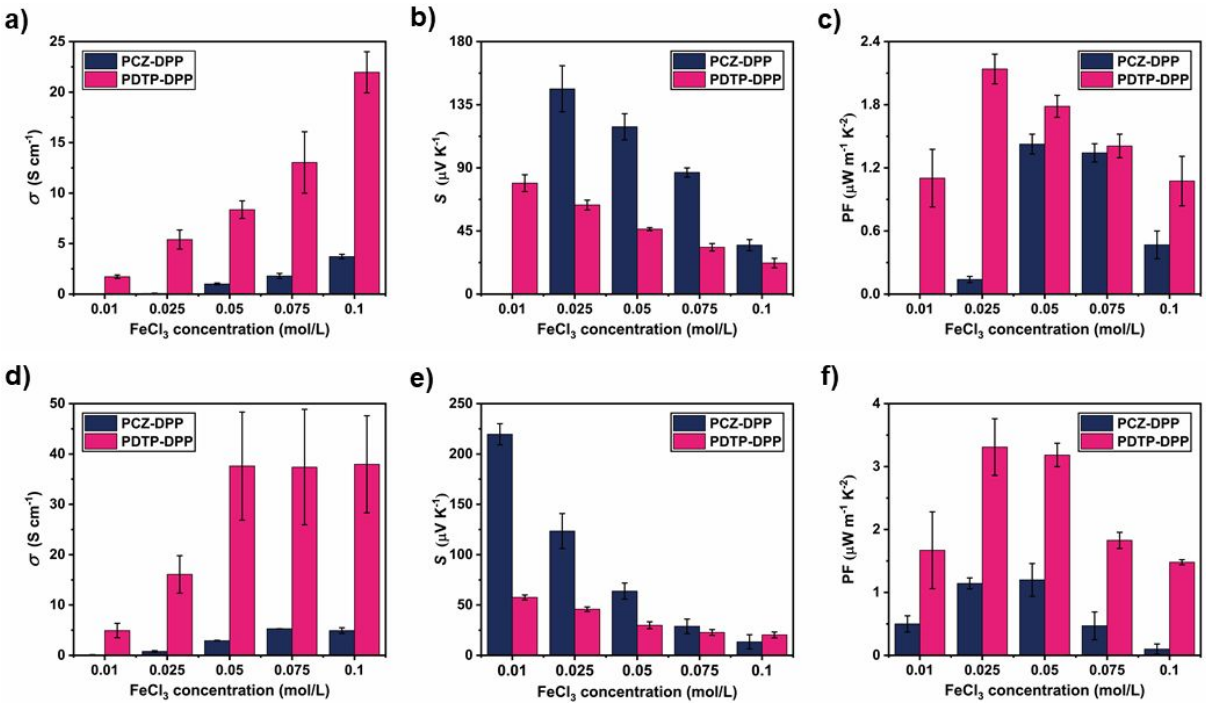

Figure S7. Thermoelectric performances of the PCZ-DPP and PDTP-DPP films, doped with different concentrations of $FeCl_3$ (0.01, 0.025, 0.05, 0.75 and 0.1 mol/L) and different times the top row for 1 min and the bottom for 5 min, a)/d) σ, b)/e) S and c)/f) PF. Notably, no valid data can be collected for PCZ-DPP films when doped with 0.01 M $FeCl_3$, 1 min, due to the low conductivity.

The temperature-dependent conductivity of the TE films.

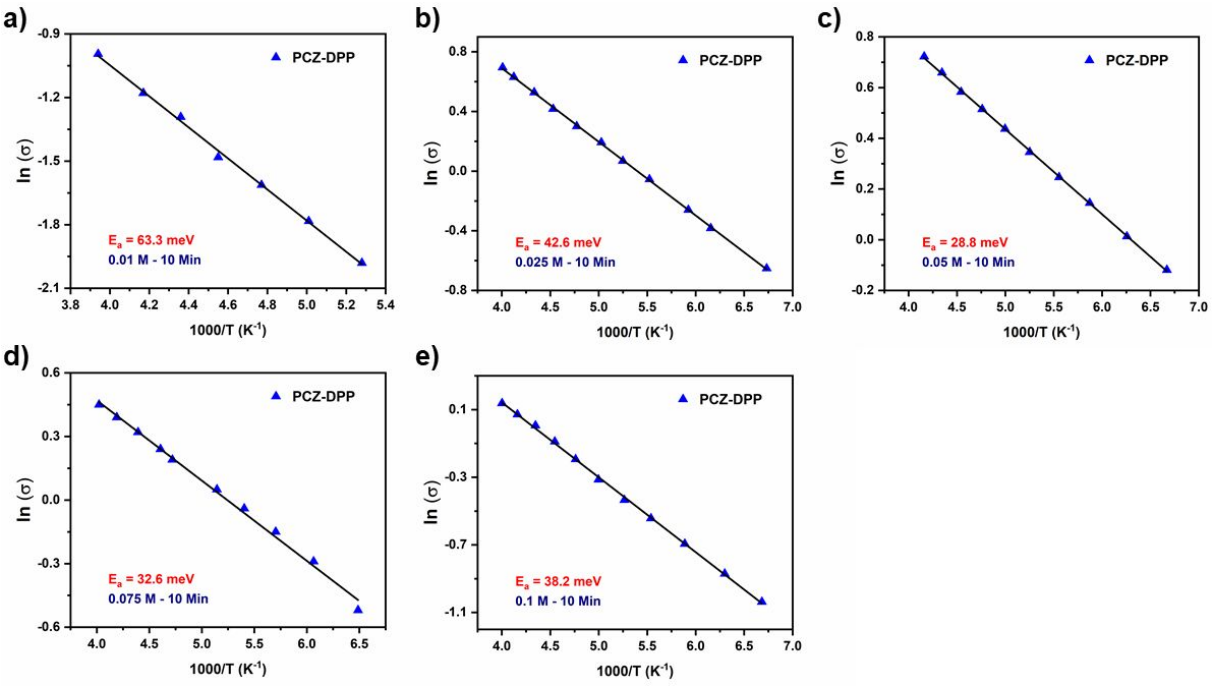

Figure S8. Temperature-dependent conductivity of the doped PCZ-DPP films at different doping levels with the temperature range of 150 ~ 250 K.

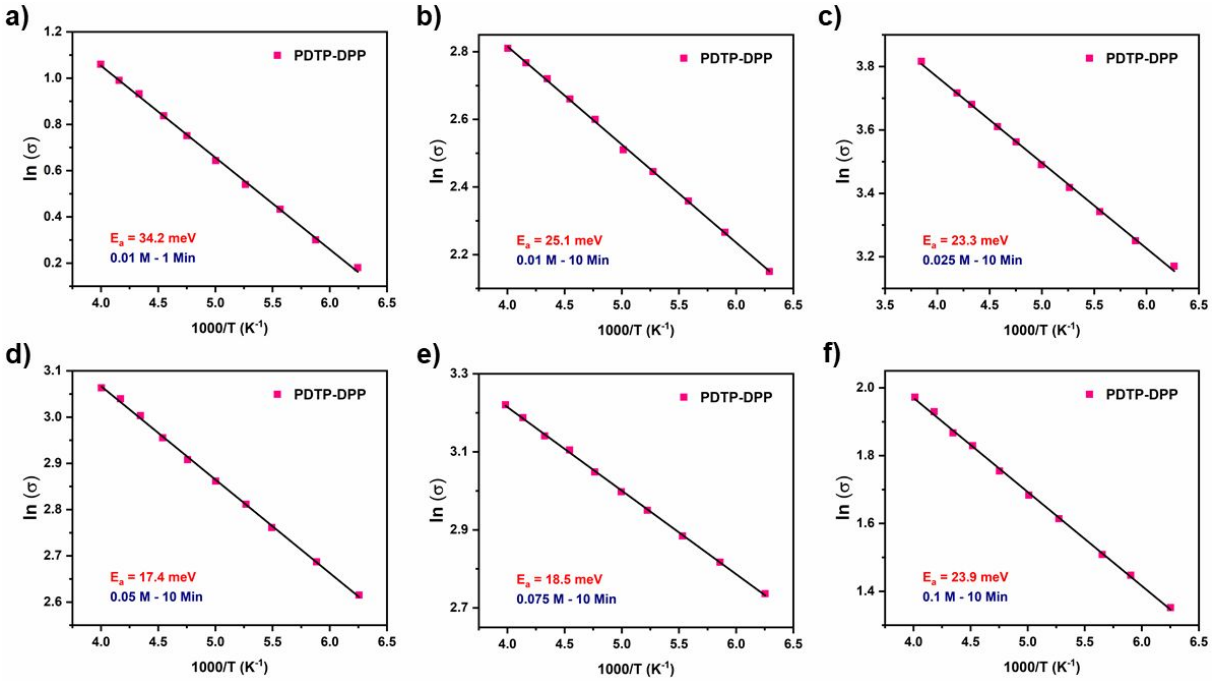

Figure S9. Temperature-dependent conductivity of the doped PDTP-DPP films at different doping levels with the temperature range of 150 ~ 250 K.

X-ray photoelectron spectroscopy (XPS) studies.

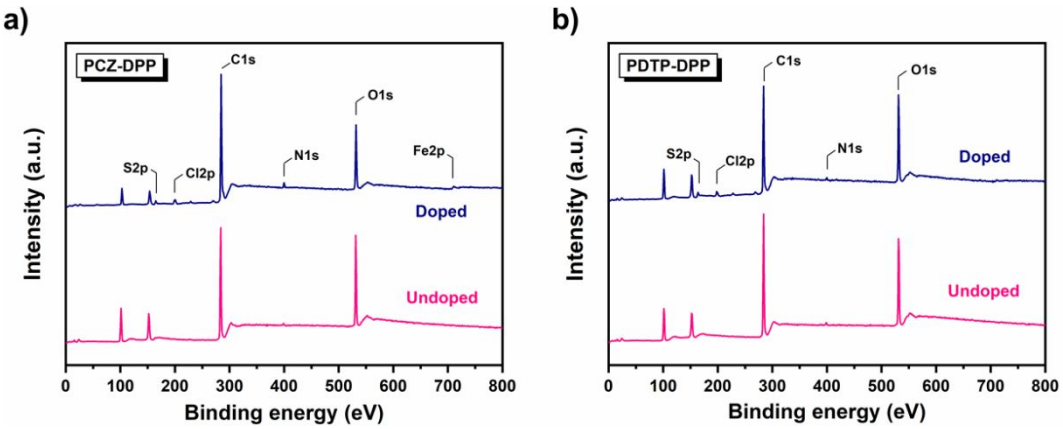

Figure S10 XPS survey scan of a) the PCZ-DPP and b) the PDTP-DPP films before and after doping with 0.025 mol/L $FeCl_3$, 10 min.

Photograph of the polymer films with different treatments.

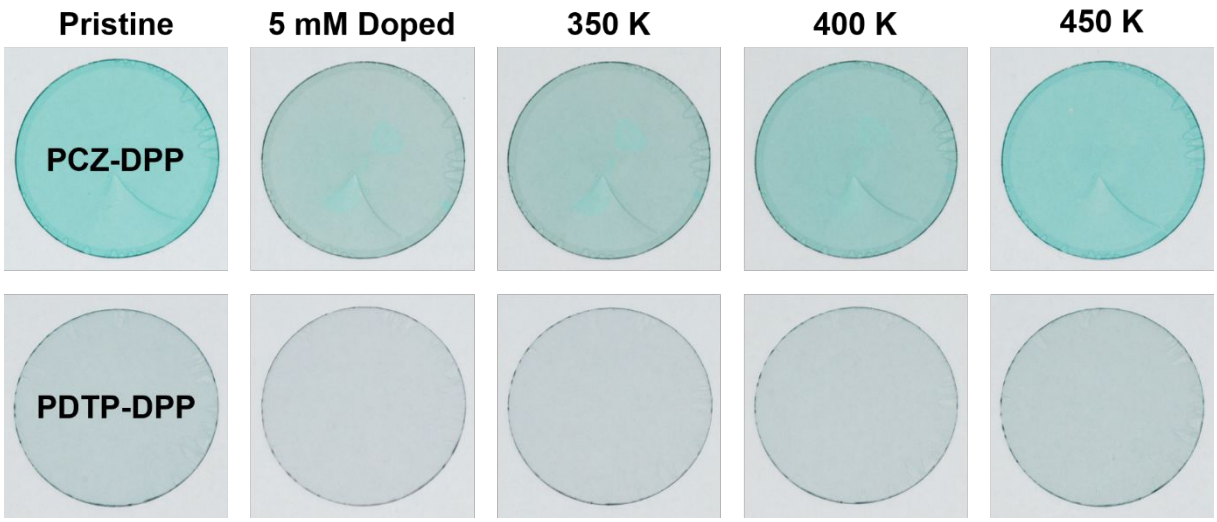

Figure S11. Digital photos of the PCZ-DPP (top) and PDTP-DPP (bottom) polymer films under different treatments.

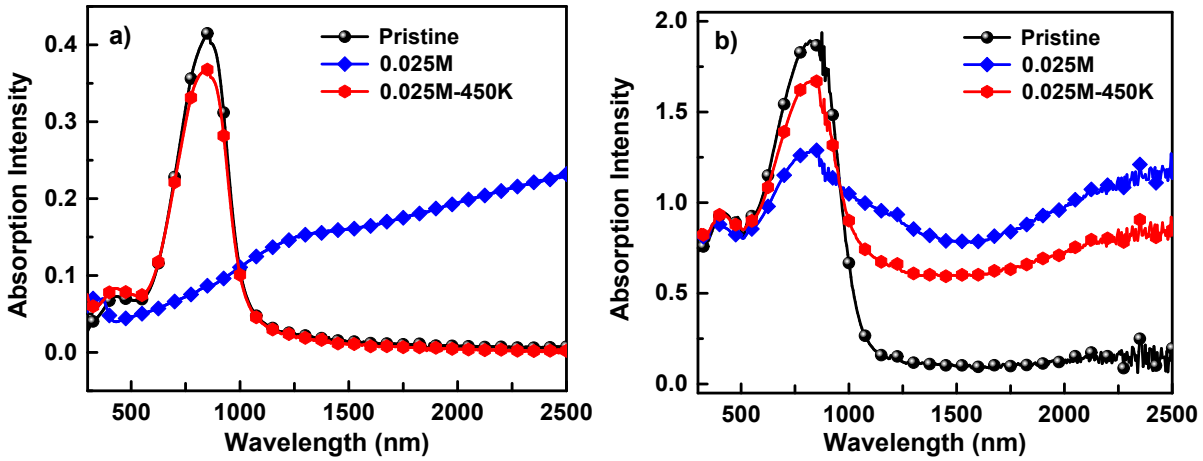

Figure S12. The UV-Vis-NIR absorption spectra of the different PDTP-DPP films doped with 0.025 mol/L $FeCl_3$, and subsequently thermal treatment at 450 K. Film a) and b) were prepared from drop-casting (5 mg/mL) and spin-casting (5 mg/mL) procedure, respectively. Notably, the stability of the doped films is largely relaying on their thickness, i.e., a weaker de-doping of the thick film sample than the thin one can be observed.

Energy dispersive spectrometer (EDS) images.

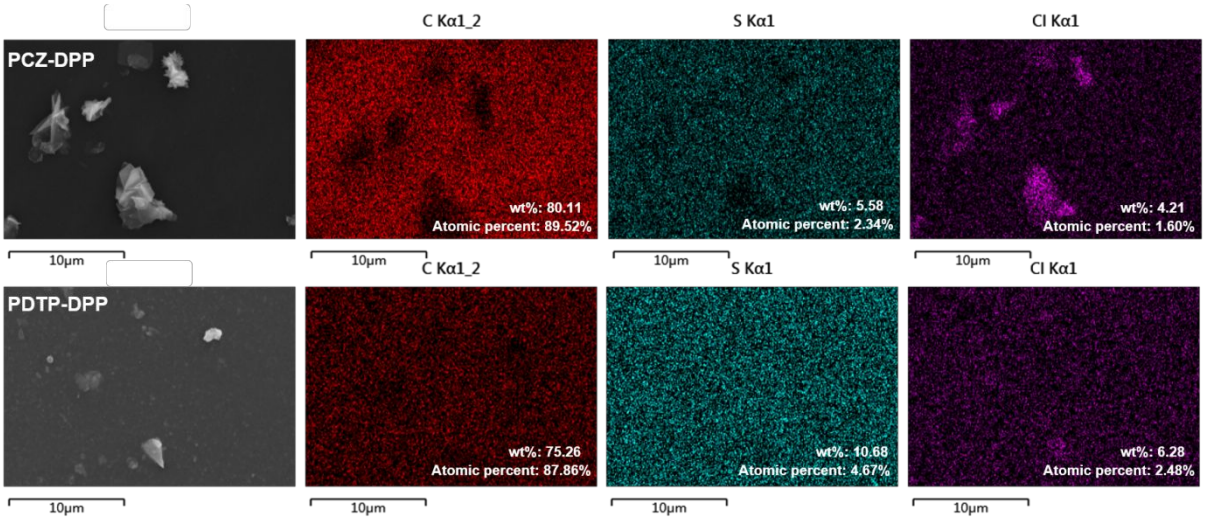

Figure S13. EDS images and the content of C, S, Cl of the PCZ-DPP (top) and the PDTP-DPP (bottom) polymer films after p-doping with 0.025 M $FeCl_3$ for 10 min.

Table S1. X-ray scattering peaks of the pristine and doped polymers from GIXRD.

Polymer	Pristine-*d*-spacing Å (100)	Doped-*d*-spacing Å (100) [a)]	Thermal-treated *d*-spacing Å (100) [b)]	Pristine-*d*-spacing Å (010)	Doped-*d*-spacing Å (010) [a)]	Thermal-treated *d*-spacing Å (010) [b)]
PCZ-DPP	20.67	21.37	20.72	3.75	3.67	3.72
PDTP-DPP	21.32	22.51	21.84	3.80	3.62	3.67

[a)]Doped with 0.025 mol/L $FeCl_3$ for 10 min, and [b)]after thermal-treatment at 350 K for 5 min.